ADVANCED REVIEW

WIREs
ENERGY AND ENVIRONMENT   WILEY

Modeling and analysis approaches for small-signal stability assessment of power-electronic-dominated systems

Marc Cheah-Mane[1] | Agusti Egea-Alvarez[2] | Eduardo Prieto-Araujo[1] |
Hasan Mehrjerdi[3] | Oriol Gomis-Bellmunt[1] | Lie Xu[2]

[1]CITCEA Group, Electrical Engineering Department, Universitat Politecnica de Catalunya, Barcelona, Spain

[2]PEDEC Group, Electronic and Electrical Engineering Department, University of Strathclyde, Glasgow, UK

[3]Department of Electrical Engineering, College of Engineering, Qatar University, Doha, Qatar

Correspondence
Oriol Gomis-Bellmunt, CITCEA group, Electrical Engineering Department, Universitat Politecnica de Catalunya, Barcelona, Spain.
Email: oriol.gomis@upc.edu

Edited by: Damian Flynn, Associate Editor and Peter Lund, Co-Editor-in-Chief

Abstract

The stability, operation, and control of power networks have been challenged due to the increased penetration of power electronic converters. New instability phenomena have appeared due to the interaction of the power converter controllers with other power network elements, including other power converters. Small-signal tools have been proved effective to identify and mitigate stability issues but their development is still ongoing. This article presents the state of the art on small-signal modeling and stability assessment of converter-dominated networks. The modeling of converters and other power system components is reviewed, as well as the most common small-signal analysis techniques employed in conventional and modern power systems with power electronics. Two case studies are introduced to exemplify the modeling and stability analysis, employing some of the techniques presented in the article.

This article is categorized under:

Energy and Power Systems > Distributed Generation

KEYWORDS
modeling, power electronics, power systems, small signal, stability

1 | INTRODUCTION

Renewable resources, high voltage direct current (HVDC), and flexible AC transmission system (FACTS) are usually interfaced using power electronic converters, introducing new challenges related to power network stability. In standard power networks, stability issues could be categorized into three main groups: rotor angle stability, frequency stability, and voltage stability but recently, IEEE has recently finished a working group on "Stability definitions and characterization of dynamic behavior in systems with high penetration of power electronic interfaced technologies" that had added a new classification for converter-based interactions (IEEE, 2020). Converter based instabilities usually involve a power converter control element interacting with another power converter control, a synchronous machine or a network passive element.

In recent years, several examples of stability related incidents with grid connected power converter units have been reported in different parts of the world. Some of the most studied are the low frequency oscillations observed in Texas and China (Fan & Miao, 2018; Liu, Xie, Gao, et al., 2018; Sun et al., 2017; Wang et al., 2015) in mid 2010s due to weak grid conditions. More recently, another incident involving an offshore wind farm occurred on August 9, 2019 in England where a lightning strike triggered a stability issue leading to the disconnection of the wind farm (National Grid ESO, 2019). Other power outages occurred after cascaded trips in South Australia in 2016 and 2018 (AEMO (2017, 2019)). These stability issues require innovative study tools as standard approaches might be inaccurate, might not capture the converter complex dynamics or require a lot of time and resources.

Power networks modeling and study tools such as root mean square (RMS) models have been proved reliable for standard power systems but might fail to predict stability in networks with high penetration of renewable power. As an example, during the commission of BowWin1 offshore wind farm, harmonic interactions appeared, as explained by Buchhagen et al. (2015), but were not detected during the study phase due to the model inaccuracy. The wind farm operation was delayed for several months until the problem was identified. Electromagnetic transient (EMT) models can capture complex dynamics but are not suited for large system models due to their mathematical complexity, high computational requirements (supercomputers or cloud simulation required), and long simulation duration. RMS and EMT models can predict the instability but can hardly provide clues of the root cause of the instability or study potential solutions.

Alternatively, small and large signal analyses have been proposed by Kundur et al. (2004a) to study the stability of electrical systems. Small-signal modeling analysis extracts the system's linear dynamic behavior and applies standard control engineering tools to assess stability and dynamic performance. Small-signal analysis only provides accurate stability assessment around the linearization point. Large-signal analysis considers a single system model valid for a large variety of operating points that might include nonlinearities. Even though large-signal might seem more convenient than small-signal, the mathematical complexity of the models and the stability assessment tools make this method difficult to apply in the everyday engineering practice. In the recent years, large-signal analyses have been suggested to study VSC synchronization methods, stability during faults, or grid-forming converters (Hu et al., 2019; Pan et al., 2019; Taul et al., 2019; Zhang et al., 2021).

Small-signal studies of classic power networks dominated by synchronous generators (SGs) has been used to identify instability sources using eigenvalues and participation factors (PFs), among others techniques. These models are usually developed using a state-space representation of the network, where generic models for the different power system elements are widely available (Kundur & Paserba, 1994). Frequency-domain techniques have been also used in conventional power systems to identify oscillatory instabilities. In particular frequency scan techniques by Annakkage et al. (2016) and Agrawal and Farmer (1979) and the complex torque coefficient method by Canay (1982) and Tabesh and Iravani (2005) were employed for subsynchronous oscillations that involve the SG. As the penetration of power electronic converters increases, it is critical to develop small-signal models of those converters (Collados-Rodriguez et al., 2019; Pico & Johnson, 2019). Unfortunately, the converter control is usually protected by intellectual property (IP) and it is particular to each manufacturer making the development of state space models difficult. The impedance modeling of power converters initially presented by Sun (2011) is seen as a promising technique for power converters as it has some advantages compared to standard small signal modeling: the impedance is a familiar quantity for electrical engineers and can be measured at the terminals of the actual power electronic converter devices without compromising IP (Dong et al., 2014).

This article presents a review of the modeling principles and analysis techniques for small-signal stability of power systems dominated by power electronic components. The importance of power electronics in modern power systems is initially introduced with examples of several power-electronic-dominated systems. The modeling principles of small-signal analysis are described with focus on the reference frames, state-space representation and linearization. Also, a literature review of the main power system models is presented, including passive components, loads, SGs, and converters. Then, small-signal stability analysis tools are described including state-space and frequency-domain analysis. Impedance-based methods are presented as specific frequency domain analysis tools. Also, promising techniques for the power system analysis with power electronics are described. Finally, two application case studies are presented as examples where some of the previous stability analysis tools are employed to identify unstable oscillatory modes.

2 | POWER-ELECTRONIC-DOMINATED SYSTEMS

The electrical power system is experiencing a deep transformation worldwide. While classic power systems were based on SGs, modern power systems are increasingly populated by power electronics based converters. Power converters

interface the main renewable energy generators, energy storage interfaces, HVDC, FACTS, electrical vehicle chargers, and industrial drives. Bidirectional AC/DC voltage source converters (VSCs) are the dominant power electronics technology, but other converter concepts that are used include: diode rectifiers, DC–DC converters in different topologies, and line commutated converters (LCCs) in current-source HVDC applications (Gomis-Bellmunt et al., 2020).

Renewable generation is one of the scenarios where power electronics plays an important role to ensure a flexible operation. Modern wind turbines are equipped with power electronics in order to provide maximized energy capture and grid friendly operation (fault ride-through and grid support). In onshore applications, the preferred technology is Type 3 wind turbines based on the doubly fed induction generator and a power converter rated at partial power rating. For offshore applications, the need to simplify or eliminate the gearbox moves the preference to medium speed or direct drive type 4 wind turbines based on a full-scale power converter, which completely decouples the generator and grid sides. Also, for offshore wind power plants connected at long distance from shore an HVDC transmission is the most cost-effective solution (Van Hertem et al., 2016). Figure 1 shows an example of an HVDC-connected offshore wind power plant. In this case, wind turbines are based on full-scale power converters, which are connected to an offshore collection grid. The collection grid is steered by an offshore HVDC rectifier, which controls the offshore grid frequency and voltage. This offshore grid is a system with 100% converter penetration.

Similar concepts are being employed in ocean generation power plants, for tidal and wave energy converters. Solar photovoltaic (PV) power plants are populated by inverters that are responsible for the DC–AC conversion and the integration of the solar generation into the power plant collection grid. As far as hydro generation is concerned, there is also interest in variable speed generation in some applications, especially for bidirectional groups in pumping operation (in order to have the possibility to dispatch the pumping power setting).

Most energy storage technologies are interfaced to the grid with power electronics, for example, electrochemical batteries or super-capacitors require DC-AC power converters and mechanical flywheels operate at variable speed and require a back to back power converter to connect to the main AC grid. On the demand side, we are also witnessing a tremendous proliferation of converter based loads. Most industrial and domestic loads are driven by frequency converters, which are interfaced to the grid with diode rectifiers or bidirectional VSCs. The electrification of mobility is also pushing the development of charging stations for electrical vehicles, based on power electronics converters.

The mass penetration of power electronics is being conducted at high, medium, and low voltage applications in transmission and distribution networks. Figure 2 exemplifies a modern transmission power system integrating a massive amount of renewable generation. The converters in the figure indicate the interconnecting converters between different HVAC and HVDC subsystems, which are responsible for power exchange between these sub-systems. AC–DC and DC–DC converters are included and are responsible to establish the power flows in the system and to control the different voltages and frequencies to the required level (Gomis-Bellmunt et al., 2021). High power converters for HVDC applications are mainly based on modular concepts like the modular multilevel converter (MMC) or classic LCC with thyristors. It can be noted that converters are also present in many of the sources and loads of the scheme.

A low voltage grid is sketched in Figure 3, including a multi-microgrid variety of energy sources and different DC and AC subsystems (Unamuno & Barrena, 2015). Two different converters are used: Green converters interconnect a
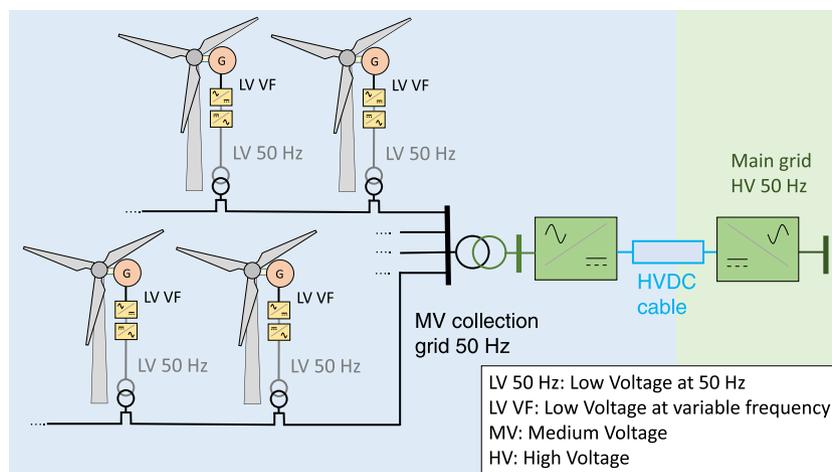

FIGURE 1 Scheme of an offshore wind power plant connected by means of high voltage direct current (HVDC) transmission
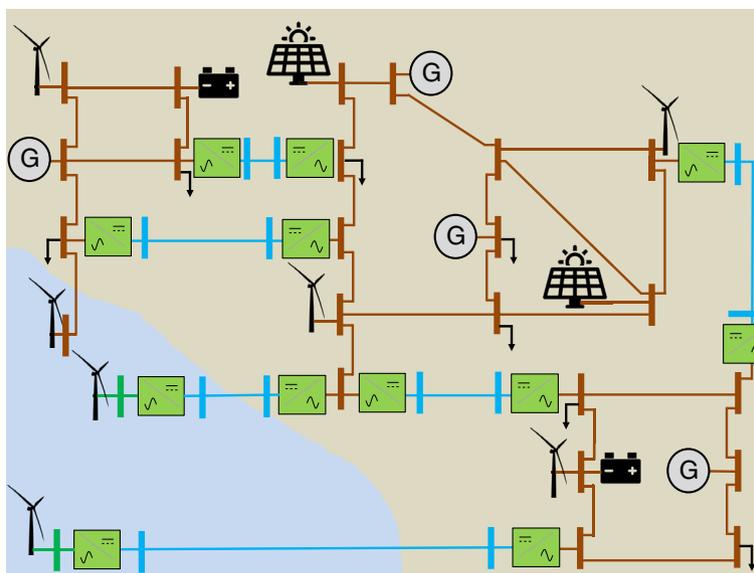
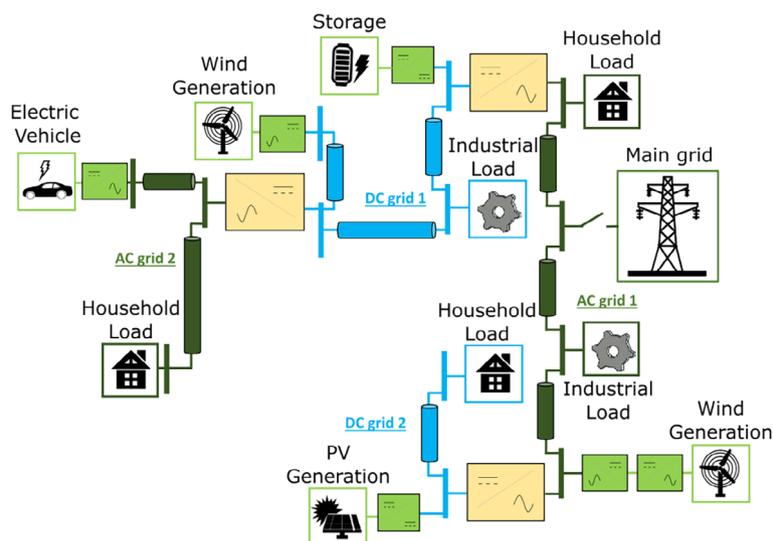**FIGURE 2** Modern power electronics dominated transmission power system

FIGURE 3 Multi-microgrid system, composed of 2 AC and 2 DC subsystems. Converters related to different devices are indicated in green, while converters used to interconnect the microgrids are indicated in yellow

given energy source or load to the system, while Yellow (larger) converters connect different subsystems. These converters can be AC–AC, DC–AC, or DC–DC, depending on the nature of the related subsystems.

The penetration of power electronics in power systems is achieving very high levels. Some applications, such as the offshore HVDC connection in three or the microgrid in Figure 1, have already achieved 100% power electronics based power systems.

This fast penetration is raising the attention of power system operators worldwide as they are required to operate power system which have fundamental differences compared to the traditional ones. The main differences are related to the inertia and overload capacity (Milano et al., 2018). SGs based power plants exhibit large inertia which is due to large rotating masses in generators and turbines. They also have important overload capability which allows for excess the nominal current during some seconds or minutes when some disturbances occur in the network. Power converters are different from SGs as they are fully controllable devices with very limited overload capability. This implies important challenges related to power system operation (related to the very low inertia) and protection (limited short-circuit current).

These important conceptual differences imply that the methodologies used to analyze classic power systems might not be appropriate to study the stability of modern power systems and can lead to misleading conclusions in some cases. The following sections of the article are centered on presenting modeling approaches and different methodologies and example applications for stability assessment of power electronic dominated systems.

3 | MODELING PRINCIPLES OF CONVERTER DOMINATED NETWORKS

This section presents the modeling principles of converter dominated networks. First, the main reference frames that can be considered to represent an electrical network are introduced. Due to the balance condition of the major part of three-phase electrical networks and the symmetry of voltages, a standard three-phase electrical system can be simplified into a two-phase system. This simplification helps to reduce the order of the equations, as well as, decouple the quantities of the network, such as the active and reactive power. Second, the general modeling approach is presented with special focus on the small-signal models and the impedance-based representation. Then, models of SGs, passive elements, loads and converters are presented. For the VSC, the two-level converter and the MMC are described.

3.1 | Reference frames

The first step in modeling electrical systems is describing the equations that relate currents and voltages in the physical world. In three-phase power networks this is called the *abc*-frame. The three main reference frames used for the study of electrical systems are the stationary reference frame or *αβ*-frame presented by Duesterhoeft et al. (1951), the synchronous reference frame or *dq*-frame presented by Park (1929) and the positive negative frame or the *pn*-frame presented by Chen et al. (2020). In standard converter control *dq*-frame and the *αβ*-frame are used due to the decoupling between active and reactive power and the ability to use standard controllers such as proportional integral (PI) or proportional resonant (PR) controllers. However, the *dq*-frame and the *αβ*-frame are not directly related to the voltage and current that can be measured from the electrical device terminals. For this reason the *pn*-frame was suggested instead. The *pn*-frame is used exclusively to analyze the impedance of the system and resembles the positive and negative impedance used in power networks short circuit analysis (Amico et al., 2019).

To transform a system described in the *abc*-frame into the *αβ*-frame the Clarke transformation by Duesterhoeft et al. (1951) is used. The Park transformation by Park (1929) allows the conversion from the *abc*-frame into the *dq*-frame. An example of the transformation of an electrical system from the *abc*-frame to *dq*-frame is presented by Levron et al. (2018). To transform a signal in the three-phase frame into the *pn*-frame the Fortescue transformation presented by Kundur and Paserba (1994), *F*, is applied. The Fortescue transformation is well known for power system engineers when performing short circuit analysis or imbalance power flow studies. Compared to Park and Clarke transformation, Fortescue is defined in the frequency-domain $j\omega$ instead of the time-domain. Usually, in standard power system analysis only one frequency is analyzed where ω is $2\pi50$ or $2\pi60$ but for stability studies a full range of frequencies is considered. An example of the modeling in the *pn*-frame is presented by Amico et al. (2019).

3.2 | Modeling of power network elements for stability studies

Modeling is the process of establishing a set of mathematical equations to describe the behavior of an electrical system. As power networks are nonlinear systems, the dynamics can be described by a set of n nonlinear differential equations as follows:

$$\dot{\mathbf{x}} = \mathbf{f}(\mathbf{x}, \mathbf{u}); \; \dot{\mathbf{y}} = \mathbf{g}(\mathbf{x}, \mathbf{u}) \tag{1}$$

where $\mathbf{x} = (x_1 \dots x_n)^T$ is the state variables vector, $\mathbf{u} = (u_1 \; \dots \; u_n)^T$ is the system inputs vector, $\dot{\mathbf{y}} = (y_1 \; \dots \; y_n)^T$ is the outputs vector, and $\boldsymbol{g}$ is a vector of nonlinear functions that relates the states and the inputs (Machowski et al., 2020).

Analysis tools for nonlinear systems, such as Lyapunov or the describing function, present certain mathematical complexity that can increase the difficulty of power network studies (Kundur et al., 2004a). An alternative is to focus on small-signal analysis and implement linear models. This implies that nonlinear system equations must be linearized

and are only valid for a limited range around the operating conditions (usually for variations of 1%). Once the system equations are linearized, standard stability criteria based on eigenvalues or Bode and Nyquist plots can be applied (Kundur et al., 2004b). Also, other indicators of the system stability can be used such as gain and phase margin and PFs.

Linearized systems are usually modeled with a state-space representation as follows:

$$\dot{\mathbf{x}} = \mathbf{A}\mathbf{x} + \mathbf{B}\mathbf{u}; \ \mathbf{y} = \mathbf{C}\mathbf{x} + \mathbf{D}\mathbf{u} \tag{2}$$

where A is the state matrix, B is the input matrix, C is the output matrix, and D is the direct transmission matrix. The state-space representation of an electrical system has been extensively used in stability and control of conventional power networks as presented by Kundur and Paserba (1994).

The impedance or admittance modeling is a particular relationship of inputs and outputs in the state-space representation that is gaining interest with the increase of power electronics elements in the network. The admittance defines a relation between currents and voltages for a specific element or part of the network such that:

$$\begin{bmatrix} i_x \\ i_y \end{bmatrix} = \begin{bmatrix} Y_{xx}(s) & Y_{xy}(s) \\ Y_{yx}(s) & Y_{yy}(s) \end{bmatrix} \begin{bmatrix} v_x \\ v_y \end{bmatrix} \tag{3}$$

where $Y(s)$ is the individual admittance transfer function, i is the current flowing through the element under study, v is the voltage at the terminals of the element and x and y are the components related to the frame under study, either the dq-frame, pn-frame, or $\alpha\beta$-frame. The inverse of the admittance matrix, called the impedance matrix $Z(s)$ can be also used. The impedance modeling results in the application of stability criteria focused on the frequency domain analysis. This representation only considers currents and voltages as variables under study, which can be limited for a global stability analysis. However, the impedance modeling is convenient for manufacturers or system operators to share information without compromising their IP.

An impedance expressed in the dq-frame can be transformed into the pn-frame according to Amico et al. (2019):

$$Y_{pp}(s) = \frac{1}{2}\left\{ \left[Y_{qq}(s-j\omega_0) + Y_{dd}(s-j\omega_0) \right] - j\left[Y_{dq}(s-j\omega_0) - Y_{qd}(s-j\omega_0) \right] \right\} \tag{4a}$$

$$Y_{pn}(s) = \frac{1}{2}\left\{ \left[Y_{qq}(s-j\omega_0) - Y_{dd}(s-j\omega_0) \right] - j\left[Y_{dq}(s-j\omega_0) + Y_{qd}(s-j\omega_0) \right] \right\} \tag{4b}$$

$$Y_{np}(s) = \frac{1}{2}\left\{ \left[Y_{qq}(s+j\omega_0) - Y_{dd}(s+j\omega_0) \right] + j\left[Y_{dq}(s+j\omega_0) + Y_{qd}(s+j\omega_0) \right] \right\} \tag{4c}$$

$$Y_{nn}(s) = \frac{1}{2}\left\{ \left[Y_{qq}(s+j\omega_0) + Y_{dd}(s+j\omega_0) \right] + j\left[Y_{dq}(s+j\omega_0) - Y_{qd}(s+j\omega_0) \right] \right\}. \tag{4d}$$

3.3 | Power system models

A modern power-electronic-dominated power system contains the following components: passive elements of the network, loads, SGs, and converter-based elements. Passive elements mainly refer to electric lines (overhead lines or cables), transformers, series or shunt capacitors, and reactors. Converter-based elements are mainly related to renewable generation, storage, HVDC, and FACTS devices.

3.3.1 | Passive elements and loads

Electric lines can be modeled with different levels of detail. A simple RL circuit is the most common approach for short distance lines and Π or T-section circuit for medium distance lines (Grainger, 1994; Kundur & Paserba., 1994;

Padiyar, 2004). Long distance lines employ detailed frequency-dependant models specially for high frequency ranges. DC cables require more detailed models for equivalent length of AC cables (or most lengths of AC line) due to the fast transients that are analyzed in DC systems (Beerten, 2016). Equivalent models based on series Π-sections are usually employed to represent the high frequency dynamics. Also, Beerten (2016) presents an equivalent Π-section model with multiple RL circuits connected in parallel and is presented as a more computationally efficient alternative compared to series-connected Π-sections.

Transformers are also modeled as RL circuits, if only the leakage inductance and copper losses are considered, or as Π or T-section circuits, if the mutual inductance and core losses are also considered (Grainger, n.d.; Kundur & Paserba., 1994). Saturation effect might be also included but this is usually not considered for small-signal analysis.

Loads in power systems analysis can be represented as power, impedance, or current-based equivalents. In particular, power-based loads model P and Q components with voltage and frequency dependency as presented by Kundur and Paserba (1994) and Padiyar (2004). For small-signal analysis voltage or frequency dependency can be neglected. In addition, other types of controllable loads or electric-motor-based loads can be considered as explained by Kundur and Paserba (1994) and Padiyar (2004).

3.3.2 | Synchronous generators

SGs are represented considering the electric circuits of the generator, the excitation system, the turbine, and the governor system (Kundur & Paserba, 1994; Padiyar, 2004). The electric circuits of the generator are represented in a *dq*-frame and include: stator windings (q and d-axis), field winding (d-axis) and damper winding (two in q-axis and one in d-axis). Also, the electric parameters present differences depending on the type of rotor (round or salient pole rotor).

The exciter is employed to regulate the voltage at the generator terminals. This includes a proportional control and the dynamics depend on the type of excitation system. Several IEEE models are defined by IEEE Standards Board (1992). The turbines are responsible for transforming the primary energy of a fuel (steam turbine) or fluid (hydraulic turbine) into mechanical energy. Dynamic models are different for steam and hydraulic turbines and more details are explained by Kundur and Paserba (1994). It should be mentioned that both the exciter and turbine have dynamics that are linearized as presented by Kundur and Paserba. (1994). The governor is used to provide frequency support and is based on a conventional frequency-power (f–p) droop control.

3.3.3 | Two-level VSC

Two-level VSCs are mainly used for low and medium voltage applications. Although the applied voltage on the AC side of the VSC is based on the discrete switching states of the transistors, for stability analysis purposes it is convenient to derive a more simplified equivalent model (Yazdani and Iravani (2010)). A simplified model can be derived by decoupling the DC and AC parts of the converter as illustrated in Figure 4 (Egea-Alvarez et al., 2012). The DC side is modeled as a controlled current source, while the AC side is modeled with a three-phase AC voltage source. This model reflects the power converter behavior at low frequencies and is therefore often referred to as a low frequency power converter model or average power converter model.
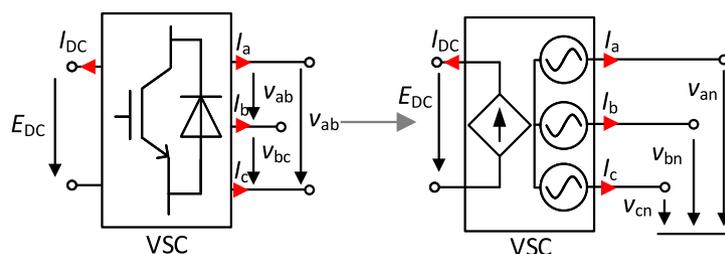

FIGURE 4 Voltage source converter (VSC) switching model (left), VSC average model (right)

The current source in the DC side reflects the active power exchanged between the AC and the DC side and assures system power balance. The DC current of the source (I_{DC}) can be computed by neglecting converter losses as the AC active power at converter terminals, P_{AC}, divided by the DC link voltage E_{DC}.

3.3.4 | MMC modeling

A particular type of power converters called, MMC is extensively used for HVDC applications and is gaining popularity in other fields including electrical drives or integration of renewables. However, due to its inherently complex behavior such as internal circulating current and submodule (SM) capacitor voltage ripple, accurately modeling is a challenging task (Jamshidifar & Jovcic, 2016; Li et al., 2018). The consequences of not modeling these aspects could lead to a displacement or deletion of frequencies of interaction and a mis-estimation of potential stability issues. The equivalent circuit of the MMC average model is depicted in Figure 5 where a lumped capacitor C_m and a voltage source are used to mimic the dynamics of each arm. $\mathbf{V}_{abc}$ and Z_g represent the grid voltage and impedance seen at the MMC AC terminals. $\Delta\mathbf{V}_{pabc}$ is a small three-phase AC perturbation voltage. $\mathbf{v}^{\Sigma}_{cuabc}$ and $\mathbf{v}^{\Sigma}_{clabc}$ are the sum of the capacitor voltages of the SMs in the upper and lower arms, respectively. The three-phase upper and lower arm currents are $\mathbf{i}_{uabc}$ and $\mathbf{i}_{labc}$, the arm voltages are $\mathbf{v}_{uabc}$ and $\mathbf{v}_{labc}$ and the modulation control signals are $\mathbf{n}_{uabc}$ and $\mathbf{n}_{labc}$. $\mathbf{v}_{gabc}$ and $\mathbf{i}_{gabc}$ are the voltage and currents on the AC side of the MMC, respectively.

For a three-phase MMC, the relationship between the arm voltage and the equivalent capacitor voltage of the SMs can be expressed using $\mathbf{n}_{uabc}$ and $\mathbf{n}_{labc}$, as:

$$\mathbf{v}_{uabc} = \mathbf{n}_{uabc}\mathbf{v}^{\Sigma}_{cuabc} \tag{5}$$

$$\mathbf{v}_{labc} = \mathbf{n}_{labc}\mathbf{v}^{\Sigma}_{luabc} \tag{6}$$

This average representation of the MMC is considered as the basic small-signal modeling of the MMC. Different approaches have been taken to model the MMC using state-space or impedance representation. Several articles have suggested different MMC small signal modeling approaches, for example using the harmonic state-space (HSS) method to consider the different harmonics circulating in the MMC in impedance form or in state space (Chen et al., 2020; Lyu et al., 2019). As an alternative, the block diagonal dominance-based model reduction is suggested by Zong et al. (2021) and other state-space representation is presented by Sánchez-Sánchez et al. (2018).
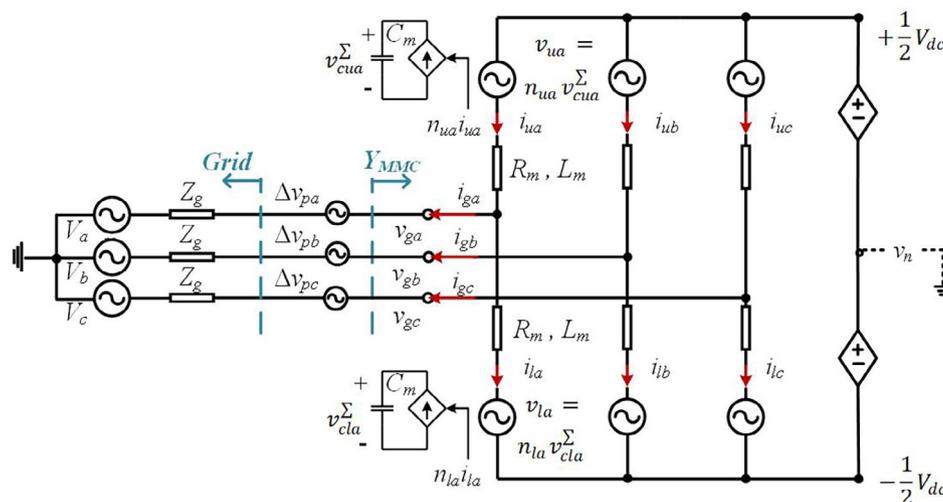

FIGURE 5 Equivalent circuit of a three-phase modular multilevel converter (MMC)

3.3.5 | Small-signal models with multiple power system components

The small-signal models of power system components are implemented in their own reference frames. However, when a power system model is considered all components must be transformed to a single reference frame. If the models are expressed in the *dq*- frame, the electrical variables, i.e. currents and voltages, are transformed between references based on an angular rotation θ^{ij} that represents the phase shift between the two references, *ri* and *rj*. An angular rotation must be completed for each separate reference frame onto the chosen common frame to ensure the alignment of all of the system components. Examples of *dq*-frame reference transformations applied for conventional and power electronics based systems are presented by Padiyar (1999), Xiao et al. (2019), and Collados-Rodriguez et al. (2019).

4 | STABILITY ANALYSIS TOOLS

4.1 | State-space analysis

4.1.1 | Eigenvalues and PFs

Eigenvalues and PFs are conventional tools used to analyze the impact of oscillatory modes in power system stability (Kundur & Paserba, 1994). The eigenvalues are obtained from the diagonalization of the state matrix *A* and provide detailed information of the oscillatory modes, such that the frequency and the damping ratio are obtained as $f = \Im(\lambda)/(2\pi)$ and $\xi = -\Re(\lambda)/|\lambda|$, where λ is the eigenvalue associated to the mode. Unstable eigenvalues are related to a negative damping, while positive values close to zero are identified as potential modes to be destabilized for different operation conditions or control parameters.

The PFs are used to define a relative relationship between state variables and modes (Kundur & Paserba, 1994). As a result, a participation matrix can be defined as:

$$\mathbf{P} = [\mathbf{P_1}, \mathbf{P_2}, ..., \mathbf{P_n}]; \ \mathbf{P_i} = [p_{1i}, p_{2i}, ..., p_{ni}]^T \tag{7}$$

where p_{ji} for $i, j = 0,...,n$ are the PFs of the state variable *j* in the mode *i*. The PFs p_{ji} provide a measure of the contribution that state variables have on each mode and vice versa. A normalization is usually applied, such that the sum of PFs for each mode or for each variable is equal to 1. This ensures a relative comparison between variables or modes.

PFs can provide an indication of interactions between components of a power system. The state variable can be grouped according to their associated components (Collados-Rodriguez et al., 2019). Then, an interaction is identified when a mode has participation from state variables of different components. However, if a coupling effect between components does not have any associated state variable, the PFs might not be used to identify interactions.

4.1.2 | Application in power-electronics-based systems

Eigenvalues and PFs have been traditionally used for the analysis of oscillatory phenomena related to rotor angle stability, voltage stability, and subsynchronous resonances (SSRs; Kundur & Paserba, 1994; Padiyar, 1999). The contribution of power electronics elements can also be analyzed with state-space analysis tools. The impact of variable speed wind turbines in interarea oscillations was presented by Du et al. (2017) and the introduction of a power oscillation damping control in a multi-terminal HVDC system was introduced by Renedo et al. (2021). In addition, eigenvalues and PFs were used for the analysis of subsynchronous torsional interactions (SSTIs) with a VSC-HVDC link as presented by Kovacevic et al. (2020), subsynchronous control interactions (SSCI) due to type 3 wind turbines as described by Suriyaarachchi et al. (2013) and Ostadi et al. (2009) and converter-driven interactions in HVDC-connected wind farms as presented by Kunjumuhammed, Pal, Gupta, et al. (2017) and networks with high penetration of VSC elements as described by Collados-Rodriguez et al. (2019).

4.2 | Frequency-domain analysis

4.2.1 | General stability analysis approach

The power system can be considered as a generic multiple-input multiple-output (MIMO) control system, where the closed-loop transfer functions are defined as $T(s) = G(s)/[1 + L(s)]$ and the open-loop transfer functions as $L(s) = G(s) H(s)$ with a matrix dimension of $m \times m$. Based on these definitions, the stability of a closed-loop system can be studied from $L(s)$. Since $L(s)$ is a MIMO system, the frequency response is analyzed from the eigenvalues λ_k for $k = 0,...,m$ of the matrix $L(j\omega)$. Then, the stability can be evaluated from the gain or phase margin and the General Nyquist Criterion (GNC) applied for each eigenvalue λ_k (Harnefors, 2007b, Skogestad & Postlethwaite, 2005). The eigenvalue analysis provides the same information about the stability conditions, since the poles of the closed-loop system $T(s)$ are equivalent to the eigenvalues of the state matrix A.

Note that the computation of $L(s)$ is required, as well as prior knowledge of the number of RHP poles in the case of the GNC. Further, a limitation of these methods is that the partial contribution of $G(s)$ and $H(s)$ on the general stability cannot be identified. In general, this approach is mainly used for a reduced MIMO system obtained from impedance models as presented in Section 4.3.

4.2.2 | Conventional methods for power systems

Frequency-domain tools have been used for the analysis of interactions in conventional power systems, focusing on instabilities in the subsynchronous frequency range due to the dynamic response of SGs. Such tools include frequency scanning methods to identify potential resonance frequencies as presented by Annakkage et al. (2016) and Agrawal and Farmer (1979) and stability evaluation methods as described by Canay (1982), Tabesh and Iravani (2005), and Tabesh and Iravani (2004).

Resonances due to self-excitation of the SG were identified with the frequency scan method presented by Agrawal and Farmer (1979), which measures the equivalent impedance from the rotor generator. The same method was also used by Suriyaarachchi et al. (2013) for induction generators in type 3 wind turbines. The unit interaction factor (UIF) method is another frequency scan procedure that was presented by Annakkage et al. (2016) to analyze torsional interactions between generator-turbines and HVDC converters, that is, SSTI. This factor considers the contribution of the device nominal powers and the short circuit powers from the buses where the devices are connected. This frequency scan method does not identify interactions due to series-connected capacitors as mentioned by Annakkage et al. (2016).

The complex torque coefficient method was presented by Canay (1982) and Tabesh and Iravani (2005), which determines stability based on the electrical and mechanical damping evaluation at the torsional frequencies. This method was proven to be related with the Nyquist criterion as described by Harnefors (2011). The torsional interactions have been also analyzed by Tabesh and Iravani (2004) directly applying the Nyquist criterion. The impact of power electronics on torsional dynamics is also analyzed by Harnefors (2007a) employing the complex torque coefficient method and the Nyquist criterion.

4.2.3 | Methods for power-electronics-based power systems

The previous conventional methods were also considered for power systems with power electronics, especially with HVDC converters. However, the main purpose was still to analyze SG-related interactions in the subsynchronous frequency range. Alternative methods have been presented in the literature to identify interactions and determine stability. A large amount of methods are based on the impedance representation of the power systems and power electronics, since this is a convenient format to share information without compromising the IP of manufacturers or system operators. All these methods are presented in Section 4.3. In addition, other methods have been explored in the recent years.

The radiality factor method is a frequency scan procedure presented by Annakkage et al. (2016) as an alternative to the UIF. This factor considers the contribution of the network and generator impedances. Compared to the UIF, this factor can be used to identify interactions due to series-connected capacitors, that is, SSR and SSCI.

The relative gain array (RGA) method identifies interactions between different control loops from the power system devices. This method is a general approach presented by Skogestad and Postlethwaite (2005), but has been suggested by

X. F. Wang et al. (2016) in the frequency domain for the interaction analysis in power systems. The RGA is defined by the ratio of an open-loop gain and a closed-loop gain depending on the inputs and outputs under study. Then, the frequency response of the RGA is evaluated to identify potential resonance interactions. This method has been presented by Dadjo Tavakoli et al. (2020) for the interaction analysis of a VSC-HVDC link.

Singular values decomposition is also presented to identify resonance interactions. The singular values provide information about how all the inputs affect the outputs at a given frequency ω. This analysis can be interpreted as the extension of the SISO frequency response analysis to MIMO systems. Here, the gain of the frequency response is replaced by the singular values and the phase is usually not analyzed (Harnefors, 2007b; Skogestad & Postlethwaite, 2005). This method has been used for the dynamic analysis of a VSC connected to the grid and a multiterminal HVDC grid (Orellana et al., 2019; Prieto-Araujo et al., 2011).

4.3 | Impedance-based stability analysis

Impedance methods are based on frequency domain analysis and consider currents and voltages as available information of the system under study. In the literature several impedance-based methods are presented, which are described in the following subsections.

4.3.1 | Impedance ratio analysis

The conventional impedance-based method divides the power system into two subsystems, the element under study, and the rest of the network. Then, the associated impedance ratio, also known as minor loop gain, represents an open-loop transfer function of the system and is used to evaluate stability (Sun, 2011). In order to apply this method, both subsystems must be independently stable.

Figure 6 shows two different impedance-based representations of the same power systems as a single-line circuit. As observed, each of these subsystems can be represented with a Thévenin (voltage source and impedance) or Norton equivalent (current source and admittance). Both representations are equivalent if $Z_2 = Y_2^{-1}$ and $I_{20} = Y_2 V_{20}$. The closed-loop system for the $Z + Y$ representation is obtained as:

$$i = \frac{Y_2}{1 + Y_2 Z_1} V_{10} - \frac{1}{1 + Y_2 Z_1} I_{20} = \frac{Y_2 V_{10} - I_{20}}{1 + Y_2 Z_1} \tag{8}$$

while the closed-loop system for the $Z + Z$ representation is obtained as:

$$i = \frac{1}{Z_1 + Z_2} V_{10} - \frac{1}{Z_1 + Z_2} V_{20} = \frac{V_{10} - V_{20}}{Z_1 + Z_2} = \frac{Y_2 V_{10} - Y_2 V_{20}}{1 + Y_2 Z_1} \tag{9}$$

where it is clear that both representations lead to the same transfer functions with impedance ratio expressed as $Y_2 Z_1$.

The relation between currents and voltages is expressed as impedance or admittance depending on the definition of inputs or outputs from the equivalent state-space model. For example, if a subsystem is represented as a Thévenin equivalent, that is, with an impedance, the currents are inputs and the voltages are outputs.
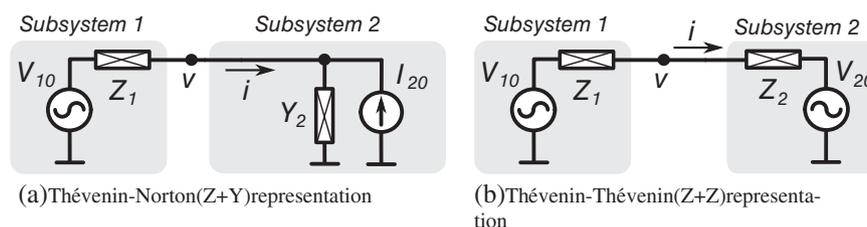

(a) Thévenin-Norton (Z+Y) representation　(b) Thévenin-Thévenin (Z+Z) representation

FIGURE 6 Impedance-based representation of a generic power systems. (a) Thévenin–Norton ($Z + Y$) representation (b) Thévenin–Thévenin ($Z + Z$) representation

Since the impedance ratio represents the open-loop system, the stability can be analyzed employing the general methods presented in Section 4.2.1, which includes the phase or gain margin and the GNC. In particular, if the impedance ratio is a 2×2 matrix, two eigenvalues, λ_1 and λ_2, are considered. If the system is close to instability, the frequency values that represent the phase and the gain margin in the Bode plots are also close to the unstable resonance frequencies (Sun, 2011; X. Wang et al., 2018). This is also equivalent to the frequencies where the Nyquist plots intersect the negative real axis (gain margin) and the unity circle (phase margin). The impedance ratio analysis provides information about stability, but with limited details about the unstable modes.

4.3.2 | Passivity analysis and positive-net-damping criterion

The concept of passivity refers to the ability of a system component to consume or dissipate energy. In particular, considering an impedance representation, a system is passive when the real part of the equivalent impedance, that is, the resistance, is non-negative for all frequencies.

In general, a linear time invariant MIMO system, defined by a $m \times m$ transfer matrix $F(s)$, is passive, if and only if, it is stable and $F(s)$ is positive semidefinite, that is, the minimum eigenvalue $\lambda_{\min}$ of $0.5[F(j\omega) + F^T(j\omega)]$ is non-negative $\forall \omega$ (Beza & Bongiorno, 2019). Note that $\lambda_{\min}$ is referred to as passivity index. Then, for the open loop system $L(s) = G(s)H(s)$, $F(s)$ could be either $G(s)$ or $H(s)$, such that the passivity-based requirement for stability is that $G(s)$ and $H(s)$ are both passive.

The passivity analysis also considers that the system is divided in two subsystems, but this method examines each subsystem independently. In case of using an impedance representation, the passivity analysis is applied to the equivalent impedances or admittances of the subsystems. For example, in Figure 6a both Y_2 and Z_1 must be passive to ensure stability (Beza & Bongiorno, 2020). If either or both of Y_2 and Z_1 are nonpassive in a frequency range, there is a risk of resonance interaction in this interval, where the stability has to be assessed using another method such as the GNC. This method gives information about the critical frequency ranges, which can be used to increase the passivity properties of each subsystem and improve overall stability. However, this criterion might consider conditions that are too conservative.

The positive-net-damping criterion was presented by Sainz et al. (2017) and Cheah-Mane et al. (2017) to provide similar information as the passivity analysis, but considering the total damping contribution of both subsystems. This stability criterion is derived from the phase and gain margin conditions and is proposed as a reformulation of the approaches presented by Canay (1982) and Harnefors (2011) for conventional power systems. However, this method is limited to harmonic frequencies, where the impedance matrix is symmetric (Sainz et al. (2017)).

4.3.3 | Additional methods based on two subsystems

The impedance ratio analysis cannot be applied if one of the subsystems is not independently stable. This is equivalent to have right-half-plane (RHP) poles in the impedance ratio. Also, the GNC cannot be applied if the impedance ratio defines an improper transfer function, that is, the order of the numerator is higher than the order of the denominator. Subsystems with a $Z + Y$ representation, as in Figure 6a, do not have RHP poles and define a proper system Liao & Wang, 2020. However, in subsystems with a $Z + Z$, as in Figure 6b, or $Y + Y$ representation, the previous conditions might not be ensured. In this case, alternative methods have been reported in the literature to evaluate the stability.

The impedance sum analysis is presented by Fangcheng et al. (2013) and F. Liu et al. (2014) as a solution for subsystems represented as $Z + Z$ and $Y + Y$. In this case, the impedance sum represents the denominator of the closed-loop system, for example, as seen in Figure 6b. Therefore, the RHP zeros of the impedance sum determine the stability, which is equivalent to evaluating the encirclements of the complex plane origin if Nyquist plots are employed (Liao and Wang (2020)). A general impedance analysis method is presented by Liao and Wang (2020), which can be applied for any impedance representation of the subsystems. This method analyses the Bode plots of each impedance or admittance independently, which provides more information about the contribution of each element to the potential instabilities.

4.3.4 | Impedance analysis methods for large systems

The impedance network modeling is presented as an alternative to deal with large and meshed systems and provides information about the frequency and damping of oscillatory modes (H. Liu & Xie, 2018; Liu, Xie, Gao, et al., 2018; Liu, Xie, & Liu, 2018). This method aggregates the power system into a lumped impedance matrix Z_Σ that represents the closed-loop system. Then, for a controllable and observable system the stability can be evaluated from the zeros of the Z_Σ determinant, which is equivalent to the closed-loop eigenvalues. This approach can be considered as an extension of the impedance sum analysis, but applied for large systems.

A frequency-domain modal analysis is also presented by Zhan et al. (2019) to deal with large systems. This method is similar to the eigenvalues and PFs analysis, but the procedure is different. In this case, the whole system is represented as a nodal admittance matrix (NAM). Then, the oscillatory modes are obtained from the zeros of the NAM determinant. The participation that each network branch and node has on the oscillatory modes is determined from the eigenvectors. However, in the PF's analysis the participation is related to the state variables.

Another similar method employing the NAM is presented by Orellana et al. (2021) to determine the most relevant harmonic frequencies and stability conditions. In this case, the harmonic frequencies are obtained based on the resonance mode analysis described by Xu et al. (2005), while the stability is evaluated considering an extension of the positive-net-damping criterion presented by Sainz et al. (2017) and Cheah-Mane et al. (2017).

4.4 | Promising analysis trends

The analysis of large power systems with high penetration of power electronics remains complex. These issues diffuse into the small-signal analysis and stability tool applications presented in the previous sections. Several options have been explored in the literature to deal with large power systems, which include the following approaches: aggregation methods and model reduction methods.

Aggregation methods have been largely used in conventional power systems. The coherency method is mainly presented used to aggregate synchronous units (Chow (2014)). A group of generators is defined as coherent when their dynamic response is the same during transient events. One technique presented by Chow (2014) is the slow coherency approach for linear systems, where the main focus is on the interarea oscillation analysis. This approach was also proposed by Chandra et al. (2016) for wind farm aggregation and the limits of this method were described by Khalil and Iravani (2018). Another simpler approach to aggregate wind farms is presented and evaluated by Kunjumuhammed, Pal, Oates et al. (2017), where the wind turbines are grouped per string in order to keep the representation of medium frequency oscillations. Also, Wang et al. (2021) presents a method to aggregate the wind farm collector grid as a radial configuration in order to facilitate the impedance-based analysis.

Model reduction methods simplify the initial power system such that the dynamic analysis is not affected. The selective modal analysis aims to reduce the state-space model keeping only the relevant modes with a high PF of the specific state variables. (Chow, 2014). This approach has been traditionally presented for conventional power systems with focus on the subsynchronous dynamics, mainly the interarea oscillations. The application of this technique in large power systems with conventional and renewable generation was presented by Kouki et al. (2020). This approach is considered by Costa et al. (2020) for SSCI analysis in wind farms with type 3 wind turbines. Another promising method based on model reduction is the networked control analysis. This technique was presented by Fan (2017) to analyze interarea oscillations with linear models. The power system is represented by a graph Laplacian matrix, which allows the decomposition of a large system into multiple small-scale systems that keep the significant dynamic characteristics. Such small-scale systems represent single components, for example, generators, or groups of components with similar characteristics. This method is used by Yang et al. (2021) to analyze interactions between grid-forming and grid-following converters.

Another important challenge in the power system analysis with power electronics is the application of mathematical techniques for nonlinear dynamics. Power electronics present a nonlinear response, particularly during transient events such as faults, due to the control saturation for converter current limitation. In general, linear models are valid for identification of oscillatory modes, but nonlinear events can also excite other interactions that cannot be captured. The existing nonlinear techniques are limited to small-size systems due to their mathematical complexity (Hu et al., 2019; Taul et al., 2019; Zhang et al., 2021). The implementation of high order models could represent a potential solution. Tian

et al. (2018) presents a third-order normal form approximation to analyze power system nonlinear dynamics. An interaction and a stability index are also proposed in the same publication.

5 | APPLICATION CASE STUDIES

5.1 | Interactions between SG and VSC

5.1.1 | Essential power systems model

An simplified model of a power system that contains a converter, a SG and a load can be used as example to identify interactions and analyze stability. Figure 7 shows the scheme of the system and more details are described by Collados-Rodriguez et al. (2019). The converter is modeled as an average model of a two-level VSC without considering the DC side. The converter control is implemented in *qd*-frame and follows a conventional structure with an inner current loop and outer loops based on active power, frequency, and AC voltage controls. A phase-locked-loop is required to track the grid angle and frequency. The SG is modeled as a round rotor generator with excitation, steam turbine, and governor systems. The line is represented with an RL circuit, while the load is considered to be active power demand modeled as a resistance.

5.1.2 | Results

The scenario under analysis considers that the converter is rated at 500 MVA, the SG at 115 MVA, and the load is 500 MW. The load is supplied considering a SG contribution of 70% of the nominal power. Then, the systems dynamics are analyzed by varying the frequency droop percentage *R* from 5% to 1%.

Figure 8 shows an eigenvalue analysis where a mode clearly moves to the unstable area when $R = 1\%$. The PFs in Table 1 show information about the two modes that present the highest damping reduction when *R* is decreased. In particular, the unstable mode corresponds to an eigenvalue with frequency around 50–70 Hz. These two modes represent interactions between the SG and the VSC, since PFs are different to zero for SG and VSC-related state variables. However, the main contribution is from SG-related state variables.

In addition, frequency domain tools based on impedance analysis can be used following the system split at bus G, as shown in Figure 9, where VSC and the line are represented as a Norton equivalent, while the SG and the load as a
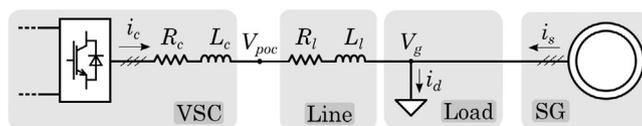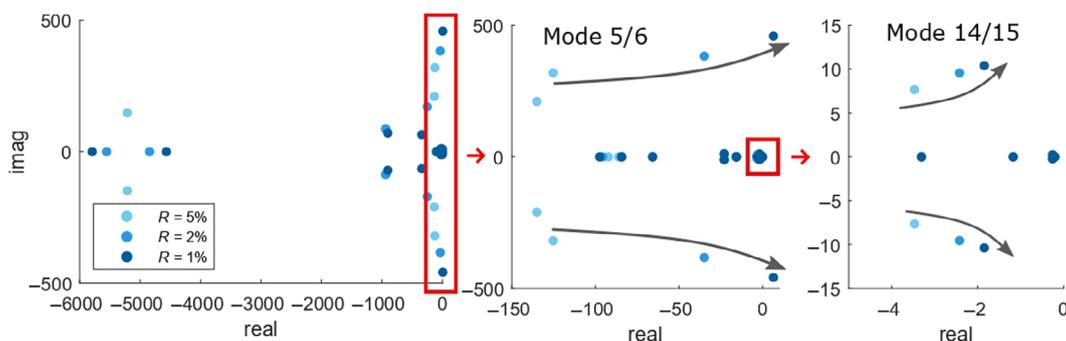

FIGURE 7 Essential model scheme

FIGURE 8 Eigenvalues of essential model example

TABLE 1 Participation factors of essential model example. Gray scale colors are used to highlight participation relevance for values above 0.3

			Mode 5/6			Mode 14/15		
			$R = 5\%$	$R = 2\%$	$R = 1\%$	$R = 5\%$	$R = 2\%$	$R = 1\%$
		f (Hz)	50.81	60.92	72.96	1.22	1.52	1.65
		damp	0.37	0.09	−0.01	0.41	0.25	0.18
		real	−125.31	−34.97	6.41	−3.47	−2.42	−1.85
VSC	PLL	e1_pll	0.09	0.12	0.12	0.00	0.00	0.00
		e_thetax	0.10	0.09	0.07	0.20	0.35	0.37
	I_{VSC}	ic_qx	0.00	0.02	0.03	0.00	0.00	0.00
		ic_dx	0.03	0.06	0.08	0.00	0.00	0.00
	I_{CTRL}	Seic_q	0.00	0.00	0.00	0.00	0.00	0.00
		Seic_d	0.00	0.00	0.00	0.00	0.00	0.00
	P_{CTRL}	Sp_unfiltered	0.00	0.00	0.00	0.02	0.02	0.01
		SerrPx	0.07	0.14	0.18	0.22	0.15	0.08
	VAC_{CTRL}	Su_unfiltered	0.00	0.00	0.00	0.00	0.00	0.00
		SerrVacx	0.00	0.00	0.00	0.01	0.01	0.01
	DELAY	delq_x	0.00	0.01	0.01	0.00	0.00	0.00
		deld_x	0.00	0.01	0.02	0.00	0.00	0.00
SG	I_{SG}	isd_x	1.00	1.00	1.00	0.99	1.00	0.79
		ikd_x	0.41	0.37	0.34	0.14	0.17	0.14
		ifd_x	0.41	0.39	0.36	1.00	0.97	0.76
		isq_x	0.97	0.71	0.90	0.13	0.77	1.00
		ikq1_x	0.13	0.09	0.12	0.02	0.12	0.16
		ikq2_x	0.75	0.54	0.69	0.11	0.66	0.85
	MECH	wg_x	0.00	0.00	0.00	0.39	0.48	0.44
		turb_x	0.00	0.00	0.00	0.00	0.00	0.00
	EXC	exc_x1	0.00	0.00	0.00	0.00	0.00	0.00
		exc_x2	0.00	0.00	0.00	0.00	0.00	0.00
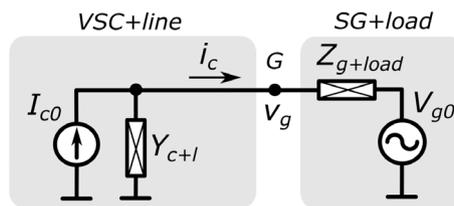
FIGURE 9 Impedance-based representation of essential model

Thévenin equivalent. The equivalent impedance $Z_{g+\text{load}}$ and admittance Y_{c+l} are expressed in *dq*-frame. Then, two techniques are employed to analyze interactions and evaluate stability: impedance ratio analysis and passivity analysis.

The Nyquist plots of the eigenvalues obtained from the impedance ratio $Y_{c+l}Z_{g+\text{load}}$ in Figure 10 clearly show that when $R = 1\%$ the system is unstable, because according to the GNC the eigenvalue λ_2 encircles the point $(-1, j_0)$ in clockwise direction. Also, the unstable oscillation frequency is approximately identified when λ_2 intersects the negative real axis, which is equivalent to the frequency where the gain margin is evaluated. In this case this frequency is identified as 66.1 Hz.

The passivity analysis of Y_c and Z_g provides additional insights on the contribution that each subsystem has on the instability. From the frequency response of the passivity index $\lambda_{\min}$ in Figure 11 it is observed that the interconnected
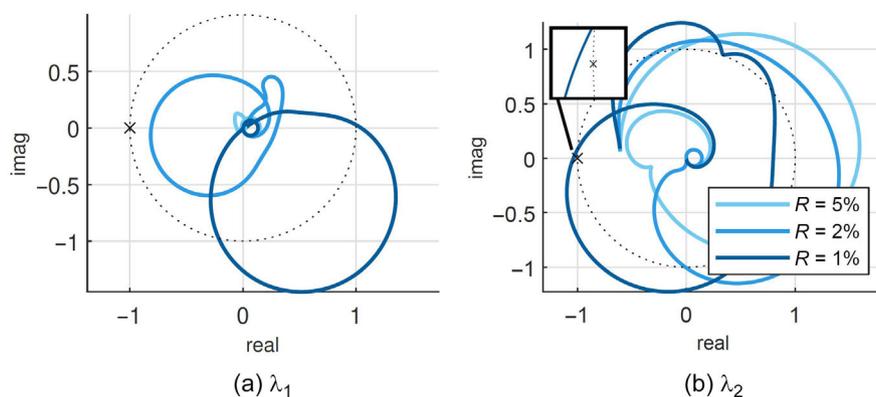
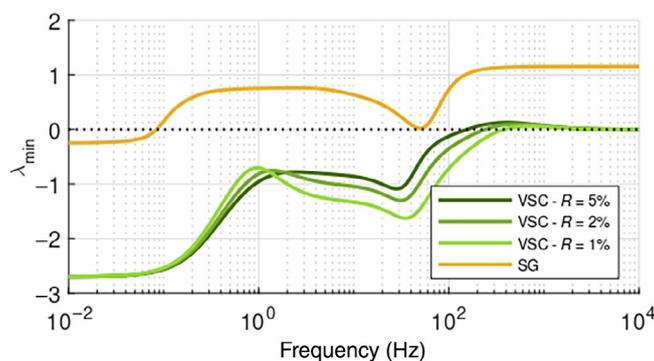**FIGURE 10** Nyquist plots of the impedance ratio eigenvalues for the essential model example (a) λ_1 (b) λ_2

FIGURE 11 Frequency response of the passivity index $\lambda_{\min}$ for the essential model example
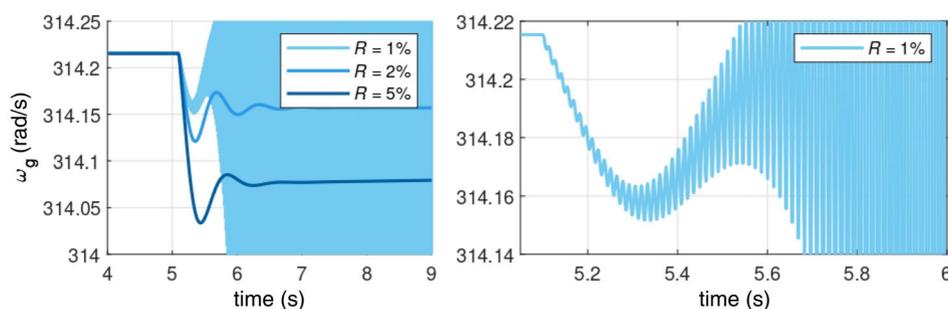

FIGURE 12 Time domain results of grid frequency ω_g for the essential model example

system is nonpassive for frequencies lower than 147 Hz ($R = 1\%$) due to the nonpassivity of the subsystem that includes the VSC and the line. This subsystem becomes nonpassive for a wider range of frequencies as R is decreased (up to 371 Hz for $R = 1\%$). This frequency range includes the unstable resonance frequency identified from the Nyquist plots. However, from the passivity criterion the frequency range of potential resonance instabilities is too wide, including both sub-synchronous and harmonic frequencies. The time-domain simulation in Figure 12 shows an unstable oscillation of 67 Hz when $R = 1\%$, which can be used to validate the results from the stability analysis tools.

5.2 | Grid-connected MMC stability assessment using MMC the impedance method

This study case is based on the average MMC representation presented in Section 3.3.4 and the impedance modeling presented by Chen et al. (2020). The example shows the resulting admittance of the MMC converter using two different

converter control strategies. The admittance model is developed in the *pn*-frame and it is validated against a real-time switching model. In addition, an initial stability assessment is presented.

To validate the obtained MMC admittance model in the *pn*-frame, the calculated values are compared to the measured impedance from equivalent time domain models using the frequency sweep method. For the MMC operating in inverter mode and importing 1 GW active power from the DC to the AC side, the small-signal Y_{pp} MMC admittances with respective PV (active power and AC voltage) and PQ (active and reactive power) controllers, and direct active and reactive current control are compared in Figure 13, with admittances from the analytical model and time domain RSCAD model. As shown in Figure 13, the admittances measured in the time-domain accord well with those derived from the MMC analytical model. The MMC admittances for PV and PQ control, and direct current control at high frequency are similar but noticeable differences can be observed in the low frequency areas. This indicates that the MMC control mode can significantly impact on system stability.

5.2.1 | Stability assessment

Using the obtained MMC admittance and the general concept of impedance based stability assessment, system stability of an MMC connected to the power network can be studied under different operating points and control modes. Figure 14 shows the simplified system configuration. The AC grid is represented by a Thévenin Equivalent composed by a voltage source V_g and the grid-side resistor R_g and inductor L_c. An AC cable connects the grid to the MMC and is represented by equivalent Π-type model and the equivalent RLC parameters. The transformer is represented by the inductor L_t.

Tests on the impact of different active power output on the system stability are carried out, and the AC grid SCR is set at 1.87. Figure 15a compares the Nyquist plots with active power of 0.5 and 1 GW using the calculated MMC impedance. As it can be seen that the system becomes unstable with 1 GW output active power while the system is stable with 0.5 GW. For the time-domain simulation shown in Figure 15b, the active power output of the MMC is ramped up from
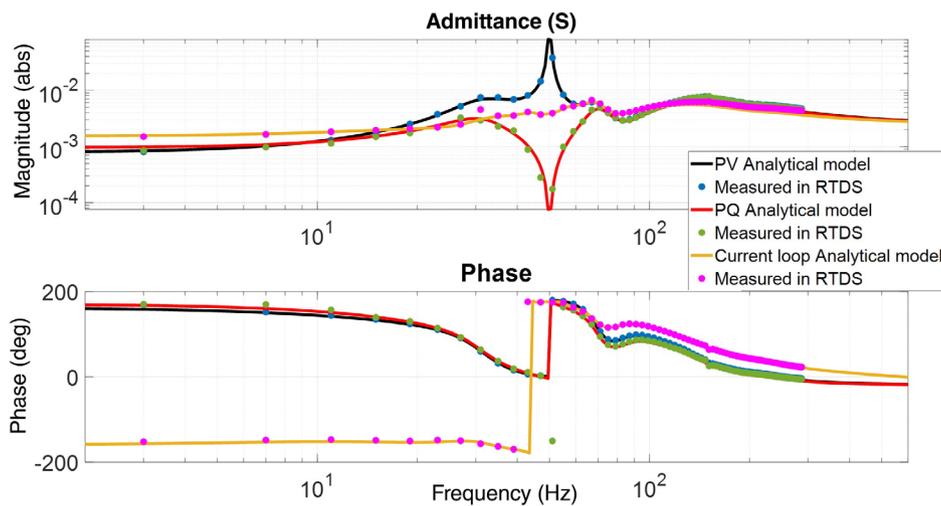

FIGURE 13 Comparison of calculated and measured Y_{pp} modular multilevel converter (MMC) admittance for different control modes
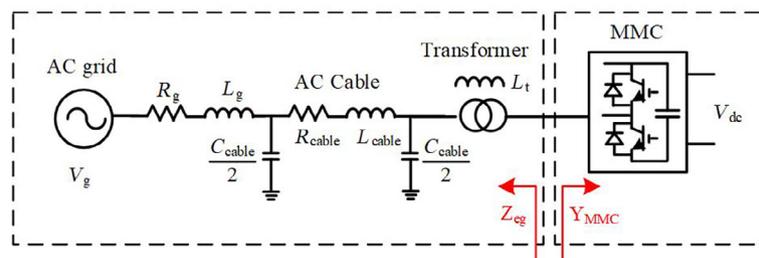

FIGURE 14 The simplified circuit for modular multilevel converter (MMC) based grid

(a) Nyquist plots with different active power   (b) Time domain simulation result
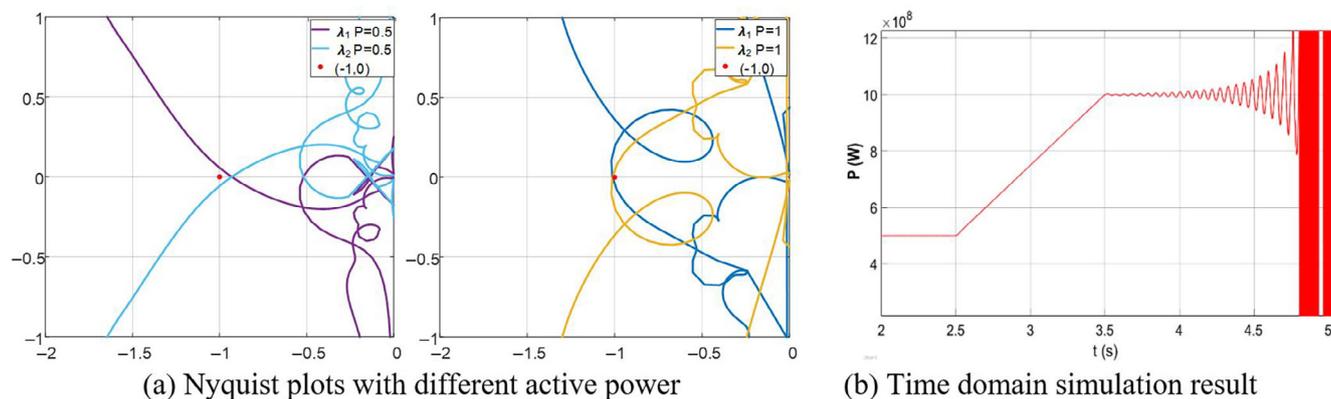
FIGURE 15 System stability with different active power

0.5 to 1 GW at 2.5 s. The system becomes oscillatory after the active power increase, which is in good agreement with the analysis in Figure 15a.

6 | CONCLUSION

This article has presented a review on modeling and stability tools for small-signal analysis of power systems dominated by power electronics. Although small-signal analysis is limited to linear or linearized models around an operation point, this approach allows employing state-space models and a large range of stability assessment techniques. Models in the *dq*-frame or the *αβ*-frame are typically used to analyze stability. Recently, models in the *pn*-frame have been employed for impedance-based analysis. Models for converters, in particular for VSCs, are simplified as low frequency or average models, which is more convenient for stability analysis and to be integrated as state-space models in power networks.

Small-signal stability analysis tools can be divided in two main groups: state-space and frequency-domain tools. Within state-space analysis, eigenvalues and PFs are the main tools to analyze stability and identify problematic modes. Although these methods are used in conventional power systems, their application in power-electronics-based systems have been also considered.

Frequency-domain analysis includes a range of tools used for synchronous-generation-based power systems, such as the complex torque coefficient method and frequency scan techniques. However, in power-electronics-based power systems additional frequency-domain tools have been developed in the recent years. In particular, impedance-based methods are presented as convenient solutions for manufacturers and system operators to share dynamic information about the converters and the network without compromising their IP. The conventional impedance-based analysis splits the system in two parts and determines stability conditions from the impedance ratio of both parts employing typical approaches, such as phase or gain margins and the General Nyquist Criterion. Similarly, other techniques such as passivity analysis or the positive-net-damping criterion consider the separate contribution of each part. Recently, impedance-based tools are dealing with larger systems and try to extract as much information as possible about the oscillatory modes.

Small-signal stability tools should be able to provide more information about the origin or mechanism of the instability rather than just evaluating stability conditions. Although state-space techniques provide more details about the instabilities, information about all power components is required, but not always available. Therefore, frequency-domain techniques, being the impedance-based analysis one of the most promising options, can be considered as an alternative. However, such frequency-domain techniques must be able to provide details of the instability with limited information about the system.

The analysis of power-electronics-based power systems must be extended for large power system. Aggregation and model reduction methods are potential options to analyze large systems with the existing small-signal stability tools. Also, additional methods to analyze nonlinear stability problems must be explored. One option suggested in the literature is the implementation of high order models.

Two case studies have shown the application of some stability analysis techniques considering power converter, SGs, and passive components such as lines or loads. Although small-signal analysis is employed to evaluate the stability conditions, time-domain simulations of nonlinear models are required for validation.

AUTHOR CONTRIBUTIONS
Marc Cheah-Mane: Conceptualization (lead); data curation (lead); formal analysis (lead); investigation (lead); methodology (lead). **Agusti Egea-Alvarez:** Conceptualization (lead); data curation (lead); formal analysis (lead); investigation (equal); methodology (equal). **Eduardo Prieto-Araujo:** Conceptualization (equal); data curation (equal); formal analysis (equal); investigation (equal); methodology (equal). **Hasan Mehrjerdi:** Data curation (supporting); funding acquisition (equal); investigation (equal); methodology (equal); project administration (equal). **Oriol Gomis-Bellmunt:** Conceptualization (equal); data curation (equal); formal analysis (equal); funding acquisition (equal); investigation (equal); methodology (equal); project administration (equal). **Lie Xu:** Conceptualization (equal); data curation (equal); formal analysis (equal); funding acquisition (equal); investigation (equal).

CONFLICT OF INTEREST
The authors have declared no conflicts of interest for this article.

DATA AVAILABILITY STATEMENT
Data available on request from the authors.

ORCID
Marc Cheah-Mane https://orcid.org/0000-0002-0942-661X
Agusti Egea-Alvarez https://orcid.org/0000-0003-1286-6699
Eduardo Prieto-Araujo https://orcid.org/0000-0003-4349-5923
Hasan Mehrjerdi https://orcid.org/0000-0001-9775-8456
Oriol Gomis-Bellmunt https://orcid.org/0000-0002-9507-8278
Lie Xu https://orcid.org/0000-0001-5633-7866

RELATED WIREs ARTICLES
Power system stability in the transition to a low

REFERENCES
AEMO. (2017). *Black system South Australia 28 September 2016* (Technical Report No. March).

AEMO. (2019). *Final report—Queensland and South Australia system separation on 25 August 2018* (Technical Report No. January).

Agrawal, B., & Farmer, R. (1979). Use of frequency scanning techniques for subsynchronous resonance analysis. *IEEE Transactions on Power Apparatus and Systems*, PAS-98(2), 341–349. https://doi.org/10.1109/TPAS.1979.319312

Amico, G., Egea-Àlvarez, A., Brogan, P., & Zhang, S. (2019). Small-signal converter admittance in the pn-frame: Systematic derivation and analysis of the cross-coupling terms. *IEEE Transactions on Energy Conversion*, 34(4), 1829–1838.

Annakkage, M. S., Karawita, C., & Annakkage, U. D. (2016). Frequency scan-based screening method for device dependent sub-synchronous oscillations. *IEEE Transactions on Power Systems*, 31(3), 1872–1878. https://doi.org/10.1109/TPWRS.2015.2442653

Beerten, J. (2016). Frequency-dependent cable modelling for small-signal stability analysis of VSC-HVDC systems. *IET Generation, Transmission & Distribution*, 10(11), 1370–1381.

Beza, M., & Bongiorno, M. (2019). Identification of resonance interactions in offshore-wind farms connected to the main grid by MMC-based HVDC system. *International Journal of Electrical Power & Energy Systems*, 111, 101–113. https://doi.org/10.1016/j.ijepes.2019.04.004

Beza, M., & Bongiorno, M. (2020). Impact of converter control strategy on low- and high-frequency resonance interactions in power-electronic dominated systems. *International Journal of Electrical Power & Energy Systems*, 120, 105978. https://doi.org/10.1016/j.ijepes.2020.105978

Buchhagen, C., Rauscher, C., Menze, A., & Jung, J. (2015). BorWin1—First experiences with harmonic interactions in converter dominated grids. In *International ETG congress 2015*; Die Energiewende-Blueprints for the new energy age, pp. 1–7.

Canay, I. M. (1982). A novel approach to the torsional interaction and electrical damping of the synchronous machine. Part I: Theory. *IEEE Transactions on Power Apparatus and Systems*, PAS-101(10), 3630–3638.

Chandra, S., Gayme, D. F., & Chakrabortty, A. (2016). Time-scale modeling of wind-integrated power systems. *IEEE Transactions on Power Systems*, 31(6), 4712–4721. https://doi.org/10.1109/TPWRS.2016.2521403

Cheah-Mane, M., Sainz, L., Liang, J., Jenkins, N., & Ugalde-Loo, C. E. (2017). Criterion for the electrical resonance stability of offshore wind power plants connected through HVDC links. *IEEE Transactions on Power Systems*, 32(6), 4579–4589. https://doi.org/10.1109/TPWRS.2017.2663111

Chen, Y., Xu, L., Egea-Álvarez, A., Marshall, B., Rahman, M., & Adeuyi, O. D. (2020). MMC impedance modelling and interaction of converters in close proximity. *IEEE Journal of Emerging and Selected Topics in Power Electronics*, 1, 7223–7236. https://doi.org/10.1109/JESTPE.2020.3031489

Chow, J. (2014). *Power system coherency and model reduction*. Springer.

Collados-Rodriguez, C., Cheah-Mane, M., Prieto-Araujo, E., & Gomis-Bellmunt, O. (2019). Stability analysis of systems with high VSC penetration: Where is the limit? *IEEE Transactions on Power Delivery*, 35(4), 2021–2031.

Costa, N. E., Revel, G., Alonso, D. M., & Fernández, R. D. (2020). Subsynchronous control interaction studies in DFIG-based wind farms using selective modal analysis. *International Journal of Electrical Power & Energy Systems*, 123, 106291. https://doi.org/10.1016/j.ijepes.2020.106291

Dadjo Tavakoli, S., Prieto-Araujo, E., Sánchez-Sánchez, E., & Gomis-Bellmunt, O. (2020). Interaction assessment and stability analysis of the MMC-based VSC-HVDC link. *Energies*, 13(8), 2075–2094. https://doi.org/10.3390/en13082075

Dong, D., Wen, B., Boroyevich, D., Mattavelli, P., & Xue, Y. (2014). Analysis of phase-locked loop low-frequency stability in three-phase grid-connected power converters considering impedance interactions. *IEEE Transactions on Industrial Electronics*, 62(1), 310–321.

Du, W., Bi, J., & Wang, H. F. (2017). Small-signal angular stability of power system as affected by grid-connected variable speed wind generators—A survey of recent representative works. *CSEE Journal of Power and Energy Systems*, 3(3), 223–231. https://doi.org/10.17775/CSEEJPES.2016.00640

Duesterhoeft, W., Schulz, M. W., & Clarke, E. (1951). Determination of instantaneous currents and voltages by means of alpha, beta, and zero components. *Transactions of the American Institute of Electrical Engineers*, 70(2), 1248–1255.

Egea-Alvarez, A., Junyent-Ferré, A., & Gomis-Bellmunt, O. (2012). Active and reactive power control of Grid connected distributed generation systems. In *Modeling and control of sustainable power systems* (pp. 47–81). Springer.

Fan, L. (2017). Interarea oscillations revisited. *IEEE Transactions on Power Systems*, 32(2), 1585–1586. https://doi.org/10.1109/TPWRS.2016.2568761

Fan, L., & Miao, Z. (2018). Wind in weak grids: 4 Hz or 30 Hz oscillations? *IEEE Transactions on Power Systems*, 33(5), 5803–5804. https://doi.org/10.1109/TPWRS.2018.2852947

Fangcheng, L., Jinjun, L., Haodong, Z., Danhong, X., Ul, H. S., & Linyuan, Z. (2013). *Stability issues of Z + Z or Y + Y type cascade system*. In *2013 IEEE energy conversion congress and exposition*, pp. 434–441. doi: https://doi.org/10.1109/ECCE.2013.6646734

Gomis-Bellmunt, O., Sánchez-Sánchez, E., Arévalo-Soler, J., & Prieto-Araujo, E. (2021). Principles of operation of grids of dc and ac subgrids interconnected by power converters. *IEEE Transactions on Power Delivery*, 36(2), 1107–1117. https://doi.org/10.1109/TPWRD.2020.3002269

Gomis-Bellmunt, O., Sau-Bassols, J., Prieto-Araujo, E., & Cheah-Mane, M. (2020). Flexible converters for meshed HVDC grids: From flexible ac transmission systems (facts) to flexible dc grids. *IEEE Transactions on Power Delivery*, 35(1), 2–15. https://doi.org/10.1109/TPWRD.2019.2939588

Grainger, J. (1994). *Power system analysis*. McGraw-Hill.

Harnefors, L. (2007a). Analysis of subsynchronous torsional interaction with power electronic converters. *IEEE Transactions on Power Systems*, 22(1), 305–313. https://doi.org/10.1109/TPWRS.2006.889038

Harnefors, L. (2007b). Modeling of three-phase dynamic systems using complex transfer functions and transfer matrices. *IEEE Transactions on Industrial Electronics*, 54(4), 2239–2248. https://doi.org/10.1109/TIE.2007.894769

Harnefors, L. (2011). Proof and application of the positive-net-damping stability criterion. *IEEE Transactions on Power Systems*, 26(1), 481–482. https://doi.org/10.1109/TPWRS.2010.2052965

Hu, Q., Fu, L., Ma, F., & Ji, F. (2019). Large signal synchronizing instability of PLL-based VSC connected to weak AC grid. *IEEE Transactions on Power Systems*, 34(4), 3220–3229.

IEEE. (2020). *Stability definitions and characterization of dynamic behavior in systems with high penetration of power electronic interfaced technologies* (Technical Report No. April).

IEEE Standards Board. (1992). *IEEE recommended practice for excitation system models for power system stability studies* (Technical Report). IEEE.

Jamshidifar, A., & Jovcic, D. (2016). Small-signal dynamic DQ model of modular multilevel converter for system studies. *IEEE Transactions on Power Delivery*, 31(1), 191–199. https://doi.org/10.1109/TPWRD.2015.2478489

Khalil, A. M., & Iravani, R. (2018). Power system coherency identification under high depth of penetration of wind power. *IEEE Transactions on Power Systems*, 33(5), 5401–5409. https://doi.org/10.1109/TPWRS.2018.2809548

Kouki, M., Marinescu, B., & Xavier, F. (2020). Exhaustive modal analysis of large-scale interconnected power systems with high power electronics penetration. *IEEE Transactions on Power Systems*, *35*(4), 2759–2768. https://doi.org/10.1109/TPWRS.2020.2969641

Kovacevic, S., Jovcic, D., Aphale, S. S., Rault, P., & Despouys, O. (2020). Analysis of potential low frequency resonance between a 1 GW MMC HVDC and a nearby nuclear generator. *Electric Power Systems Research*, *187*, 106491. https://doi.org/10.1016/j.epsr.2020.106491

Kundur, P., Paserba, J., Ajjarapu, V., Andersson, G., Bose, A., Canizares, C., Hatziargyriou, N., Hill, D., Stankovic, A., Taylor, C., Van Cutsem, T., & Vittal, V. (2004a). Definition and classification of power system stability. *IEEE Transactions on Power Systems*, *19*(2), 1387–1401. https://doi.org/10.1109/TPWRS.2005.861994

Kundur, P., Paserba, J., Ajjarapu, V., Andersson, G., Bose, A., Canizares, C., Hatziargyriou, N., Hill, D., Stankovic, A., Taylor, C., Van Cutsem, T., & Vittal, V. (2004b). Definition and classification of power system stability IEEE/CIGRE joint task force on stability terms and definitions. *IEEE Transactions on Power Systems*, *19*(3), 1387–1401.

Kundur, P., & Paserba, J. (1994). *Power system stability and control*. McGraw-Hill.

Kunjumuhammed, L. P., Pal, B. C., Gupta, R., & Dyke, K. J. (2017). Stability analysis of a PMSG-based large offshore wind farm connected to a VSC-HVDC. *IEEE Transactions on Energy Conversion*, *32*(3), 1166–1176. https://doi.org/10.1109/TEC.2017.2705801

Kunjumuhammed, L. P., Pal, B. C., Oates, C., & Dyke, K. J. (2017). The adequacy of the present practice in dynamic aggregated modeling of wind farm systems. *IEEE Transactions on Sustainable Energy*, *8*(1), 23–32. https://doi.org/10.1109/TSTE.2016.2563162

Levron, Y., Belikov, J., & Baimel, D. (2018). A tutorial on dynamics and control of power systems with distributed and renewable energy sources based on the DQ0 transformation. *Applied Sciences*, *8*(9), 1661–1709. https://doi.org/10.3390/app8091661

Li, Y., Tang, G., Ge, J., He, Z., Pang, H., Yang, J., & Wu, Y. (2018). Modeling and damping control of modular multilevel converter based DC grid. *IEEE Transactions on Power Systems*, *33*(1), 723–735. https://doi.org/10.1109/TPWRS.2017.2691737

Liao, Y., & Wang, X. (2020). Impedance-based stability analysis for interconnected converter systems with open-loop RHP poles. *IEEE Transactions on Power Electronics*, *35*(4), 4388–4397. https://doi.org/10.1109/TPEL.2019.2939636

Liu, F., Liu, J., Zhang, H., & Xue, D. (2014). Stability issues of z + z type cascade system in hybrid energy storage system (HESS). *IEEE Transactions on Power Electronics*, *29*(11), 5846–5859. https://doi.org/10.1109/TPEL.2013.2295259

Liu, H., & Xie, X. (2018). Impedance network modeling and quantitative stability analysis of sub-/super-synchronous oscillations for large-scale wind power systems. *IEEE Access*, *6*, 34431–34438. https://doi.org/10.1109/ACCESS.2018.2849830

Liu, H., Xie, X., Gao, X., Liu, H., & Li, Y. (2018). Stability analysis of SSR in multiple wind farms connected to series-compensated systems using impedance network model. *IEEE Transactions on Power Systems*, *33*(3), 3118–3128. https://doi.org/10.1109/TPWRS.2017.2764159

Liu, H., Xie, X., & Liu, W. (2018). An oscillatory stability criterion based on the unified DQ-frame impedance network model for power systems with high-penetration renewables. *IEEE Transactions on Power Systems*, *33*(3), 3472–3485. https://doi.org/10.1109/TPWRS.2018.2794067

Lyu, J., Zhang, X., Cai, X., & Molinas, M. (2019). Harmonic state-space based small-signal impedance modeling of a modular multilevel converter with consideration of internal harmonic dynamics. *IEEE Transactions on Power Electronics*, *34*(3), 2134–2148. https://doi.org/10.1109/TPEL.2018.2842682

Machowski, J., Lubosny, Z., Bialek, J. W., & Bumby, J. R. (2020). *Power system dynamics: Stability and control*. John Wiley & Sons.

Milano, F., Dörfler, F., Hug, G., Hill, D. J., & Verbič, G. (2018). Foundations and challenges of low-inertia systems. In *2018 power systems computation conference (PSCC)*, pp. 1–25.

National Grid ESO. (2019). *Technical report on the events of 9 August 2019* (Technical Report No. September).

Orellana, L., Prieto-Araujo, E., Sainz, L., Cheah-Mane, M., & Gomis-Bellmunt, O. (2019). On resonance instabilities in VSCs connected to weak grids. In *CIGRE symposium Aalborg 2019*. Aalborg, pp. 1–11.

Orellana, L., Sainz, L., Prieto-Araujo, E., & Gomis-Bellmunt, O. (2021). Stability assessment for multi-infeed grid-connected VSCs modeled in the admittance matrix form. *IEEE Transactions on Circuits and Systems I: Regular Papers*, *68*(9), pp. 3758–3771. doi: https://doi.org/10.1109/TCSI.2021.3091938

Ostadi, A., Yazdani, A., & Varma, R. K. (2009). Modeling and stability analysis of a DFIG-based wind-power generator interfaced with a series-compensated line. *IEEE Transactions on Power Delivery*, *24*(3), 1504–1514. https://doi.org/10.1109/TPWRD.2009.2013667

Padiyar, K. (1999). *Analysis of subsynchronous resonance in power systems*. Springer.

Padiyar, K. (2004). *Power system dynamics: Stability and control*. Anshan.

Pan, D., Wang, X., Liu, F., & Shi, R. (2019). Transient stability of voltage-source converters with grid-forming control: A design-oriented study. *IEEE Journal of Emerging and Selected Topics in Power Electronics*, *8*(2), 1019–1033.

Park, R. H. (1929). Two-reaction theory of synchronous machines generalized method of analysis-part i. *Transactions of the American Institute of Electrical Engineers*, *48*(3), 716–727.

Pico, H. N. V., & Johnson, B. B. (2019). Transient stability assessment of multi-machine multi-converter power systems. *IEEE Transactions on Power Systems*, *34*(5), 3504–3514.

Prieto-Araujo, E., Bianchi, F. D., Junyent-Ferre, A., & Gomis-Bellmunt, O. (2011). Methodology for droop control dynamic analysis of multi-terminal VSC-HVDC grids for offshore wind farms. *IEEE Transactions on Power Delivery*, *26*(4), 2476–2485. https://doi.org/10.1109/TPWRD.2011.2144625

Renedo, J., Garcia-Cerrada, A., Rouco, L., & Sigrist, L. (2021). Coordinated design of supplementary controllers in VSC-HVDC multi-terminal systems to damp electromechanical oscillations. *IEEE Transactions on Power Systems*, *36*(1), 712–721. https://doi.org/10.1109/TPWRS.2020.3003281

Sainz, L., Cheah-Mane, M., Monjo, L., Liang, J., & Gomis-Bellmunt, O. (2017). Positive-net-damping stability criterion in grid-connected VSC systems. *IEEE Journal of Emerging and Selected Topics in Power Electronics*, *5*(4), 1499–1512. https://doi.org/10.1109/JESTPE.2017.2707533

Sánchez-Sánchez, E., Prieto-Araujo, E., Junyent-Ferré, A., & Gomis-Bellmunt, O. (2018). Analysis of MMC energy-based control structures for VSC-HVDC links. *IEEE Journal of Emerging and Selected Topics in Power Electronics*, *6*(3), 1065–1076. https://doi.org/10.1109/JESTPE.2018.2803136

Skogestad, S., & Postlethwaite, I. (2005). *Multivariable feedback control: Analysis and design*. Wiley.

Sun, J. (2011). Impedance-based stability criterion for grid-connected inverters. *IEEE Transactions on Power Electronics*, *26*(11), 3075–3078. https://doi.org/10.1109/TPEL.2011.2136439

Sun, J., Li, M., Zhang, Z., Xu, T., He, J., Wang, H., & Li, G. (2017). Renewable energy transmission by HVDC across the continent: System challenges and opportunities. *CSEE Journal of Power and Energy Systems*, *3*(4), 353–364. https://doi.org/10.17775/CSEEJPES.2017.01200

Suriyaarachchi, D. H. R., Annakkage, U. D., Karawita, C., & Jacobson, D. A. (2013). A procedure to study sub-synchronous interactions in wind integrated power systems. *IEEE Transactions on Power Systems*, *28*(1), 377–384. https://doi.org/10.1109/TPWRS.2012.2204283

Tabesh, A., & Iravani, R. (2004). Frequency-response analysis of torsional dynamics. *IEEE Transactions on Power Systems*, *19*(3), 1430–1437. https://doi.org/10.1109/TPWRS.2004.831684

Tabesh, A., & Iravani, R. (2005). On the application of the complex torque coefficients method to the analysis of torsional dynamics. *IEEE Transactions on Energy Conversion*, *20*(2), 268–275. https://doi.org/10.1109/TEC.2005.847970

Taul, M. G., Wang, X., Davari, P., & Blaabjerg, F. (2019). An overview of assessment methods for synchronization stability of grid-connected converters under severe symmetrical grid faults. *IEEE Transactions on Power Electronics*, *34*(10), 9655–9670.

Tian, T., Kestelyn, X., Thomas, O., Amano, H., & Messina, A. R. (2018). An accurate third-order normal form approximation for power system nonlinear analysis. *IEEE Transactions on Power Systems*, *33*(2), 2128–2139. https://doi.org/10.1109/TPWRS.2017.2737462

Unamuno, E., & Barrena, J. A. (2015). Hybrid AC/DC microgrids—Part I: Review and classification of topologies. *Renewable and Sustainable Energy Reviews*, *52*, 1251–1259. https://doi.org/10.1016/j.rser.2015.07.194

Van Hertem, D., Gomis-Bellmunt, O., & Liang, J. (2016). *HVDC grids: For offshore and supergrid of the future*. Wiley.

Wang, C., Wang, Z., Wu, Q., & Xin, H. (2021). An improved impedance/admittance analysis method considering collector subsystem transformation in converter-integrated power systems. *IEEE Transactions on Power Systems*, *36*(6), 5963–5966. https://doi.org/10.1109/TPWRS.2021.3107715

Wang, L., Xie, X., Jiang, Q., Liu, H., Li, Y., & Liu, H. (2015). Investigation of SSR in practical DFIG-based wind farms connected to a series-compensated power system. *IEEE Transactions on Power Systems*, *30*(5), 2772–2779. https://doi.org/10.1109/TPWRS.2014.2365197

Wang, X., Harnefors, L., & Blaabjerg, F. (2018). Unified impedance model of grid-connected voltage-source converters. *IEEE Transactions on Power Electronics*, *33*(2), 1775–1787. https://doi.org/10.1109/TPEL.2017.2684906

Wang, X. F., Yang, L., Du, W. J., Wang, H. F., & Fan, L. L. (2016). Control interactions between the HVDC and UPFC by use of the RGA. In *12th IET international conference on AC and DC power transmission (ACDC 2016)*. pp. 1–5. doi: https://doi.org/10.1049/cp.2016.0472

Xiao, Q., Mattavelli, P., Khodamoradi, A., & Tang, F. (2019). Analysis of transforming DQ impedances of different converters to a common reference frame in complex converter networks. *CES Transactions on Electrical Machines and Systems*, *3*(4), 342–350. https://doi.org/10.30941/CESTEMS.2019.00046

Xu, W., Huang, Z., Cui, Y., & Wang, H. (2005). Harmonic resonance mode analysis. *IEEE Transactions on Power Delivery*, *20*(2), 1182–1190. https://doi.org/10.1109/TPWRD.2004.834856

Yang, C., Huang, L., Xin, H., & Ju, P. (2021). Placing grid-forming converters to enhance small signal stability of PLL-integrated power systems. *IEEE Transactions on Power Systems*, *36*(4), 3563–3573. https://doi.org/10.1109/TPWRS.2020.3042741

Yazdani, A., & Iravani, R. (2010). *Voltage-sourced converters in power systems: Modeling, control, and applications*. John Wiley & Sons.

Zhan, Y., Xie, X., Liu, H., Liu, H., & Li, Y. (2019). Frequency-domain modal analysis of the oscillatory stability of power systems with high-penetration renewables. *IEEE Transactions on Sustainable Energy*, *10*(3), 1534–1543. https://doi.org/10.1109/TSTE.2019.2900348

Zhang, Z., Schuerhuber, R., Fickert, L., Katrin, F., Guochu, C., & Yongming, Z. (2021). Domain of attractions estimation for grid connected converters with phase-locked loop. *IEEE Transactions on Power Systems*, *37*(2), 1351–1362.

Zong, H., Zhang, C., Lyu, J., Cai, X., & Molinas, M. (2021). Block diagonal dominance-based model reduction method applied to MMC asymmetric stability analysis. *IEEE Transactions on Energy Conversion*, *1*, 2438–2451. https://doi.org/10.1109/TEC.2021.3054925